

Influence Analysis of mm-Wave DUT Mounting Fixture in 5G OTA Measurement

Xudong An¹, Meijun Qu², Siting Zhu¹, and Xiaochen Chen^{1*}

¹ China Telecommunication Technology Labs
China Academy of Information and Communications Technology, Beijing 100191 China
*chenxiaochen@caict.ac.cn

² School of Information and Communication Engineering
Communication University of China, Beijing 100024 China
qumeijun@cuc.edu.cn

Abstract — All of the test cases in the current version of TR 38.810 in 3GPP and CTIA millimeter-Wave (mm-Wave) test plan are limited to the free space configuration. However, the truly free-space condition does not exist for mm-Wave testing of 5G user equipment since no device can float in the air. Mounting fixtures and supporting structures are needed to fix the device under test (DUT) and move it in two axes. The influence of mounting fixture on 5G mm-Wave wireless device performance is analyzed in this paper. First, a common 4×1 patch array at 28 GHz is simulated as the performance baseline. Various mounting fixture thickness & various spacing between the DUT and the mounting fixture are simulated to get a quick understanding of the mounting fixture's influence on DUT performance. In different configurations, the working frequency of the antenna would have different degrees of deviation, while the gain could decrease or increase accordingly. Then, to explain these phenomena, an equivalent circuit is extracted utilizing the transmission line theory. Finally, according to the findings, it is recommended that the thickness of the mounting structure should be equal to an integer time of 0.5 λ_g to minimize the impact of the fixture for practical mounting structure design.

Index Terms — 5G, effect, millimeter-wave, mounting fixture, OTA.

I. INTRODUCTION

The technology of mm-Wave is the key contributor to achieve high-data-rate transmission in 5G. The high channel capacity resulting from the high frequency could support the enhanced mobile broadband (eMBB) scenario [1-2]. Antenna size is inversely proportional to the frequency, thus high-gain phased array antennas with small element-element spacing can be tightly packed within the 5G mm-Wave wireless device. Note that completely integrated solutions with modems, antenna

and radio frequency (RF) front-end become the cornerstones of 5G deployment [3-4]. Nevertheless, the antenna is inaccessible for connecting any physical cable to the test equipment due to the high level of integration [5-6]. Therefore, over-the-air (OTA) testing becomes mandatory for all 5G FR2 wireless devices.

Given the system constraints for both direct far field (DFF) and compact antenna test range (CATR) methods, the majority of mm-Wave OTA measurement systems are combined-axis systems which require a fixture to mount and rotate the device under test (DUT) to perform full spherical scans. For traditional sub-6 GHz OTA testing where the integrated power metrics of total radiated power (TRP) and total isotropic sensitivity (TIS) are the key performance indicators (KPIs) of interest, the impact of the mounting fixture can be ignored as long as it is made of low dielectric materials. For mm-Wave bands, cellular phones realize isotropic spherical coverage by using several beam-forming antenna modules, the OTA testing process and KPIs will be considerably different from that for traditional sub-6 GHz OTA testing. Since the size of the fixture is comparable with the wavelength in mm-Wave band, even if the mounting fixtures can be assumed to be lossless, the phase change introduced by propagating through even several millimeters of dielectric material can result in a significant change of the measured pattern. Due to the significantly different electromagnetic behaviors in mm-Wave band from those in LTE or sub-6 GHz ones, the current common dielectric materials used as "RF transparent" support structures should be rechecked and redesigned so that accurate measurements can be obtained. Typical KPIs for 5G mm-Wave wireless devices include radiation pattern, effective isotropic radiation power (EIRP), TRP, and effective isotropic sensitivity (EIS). These metrics are closely related.

In this paper, we mainly analyze the influence of mounting fixture on 5G mm-Wave wireless device

performance. The combination of various thicknesses and space between DUT and the mounting structure are simulated and the impacts of which are compared. The influence mechanism and principle are also explained in detail.

II. IMPACT ANALYSIS OF MILLIMETER-WAVE DUT MOUNTING FIXTURE

To analyze the impact of the mounting fixture on the mm-Wave DUT radiation performance, a common 4×1 patch antenna array working at 28 GHz is designed in Fig. 1 (b) as the performance baseline representing typical array sizes expected to be implemented in common cellular phones specified in 3GPP TR 38.810. The simulated antenna array is printed on a Rogers RO4003 substrate with the thickness of 0.35mm and size of 40×40 mm². The center-to-center spacing between adjacent elements is set to half wavelength in free space (FS) at 28 GHz. A layer of medium with the same size as the array substrate and the dielectric constant of 3.0 is introduced to imitate the mounting fixture material so that the material loading effect on the radiation performance can be well investigated. Fixture and the gap between the fixture and the mm-Wave antenna can be modeled as 2-layered dielectric materials from Fig. 1 (a) with the thickness of T and D , dielectric constant of ϵ_1 and ϵ_2 , respectively.

Combinations of various medium thickness and spacing between the antenna array and the fixture are considered and simulated for analysis. For better understanding, the fixture thicknesses (T) are set to 1.55 mm, 3.1 mm, 4.65 mm, and 6.2 mm, corresponding to $0.25 \lambda_g$, $0.5 \lambda_g$, $0.75 \lambda_g$ and $1 \lambda_g$ at 28 GHz, respectively. The spacing (D) is set to 0 mm, 2.68 mm, 5.35 mm, 8.0 mm, and 10.17 mm, corresponding to 0, $0.25 \lambda_0$, $0.5 \lambda_0$, $0.75 \lambda_0$ and $1 \lambda_0$ at 28 GHz, respectively. The phased array is set to radiate only in its normal direction for simplicity.

The reflection coefficients and radiation patterns for different thicknesses (T) and spacing (D) are shown in Figs. 2-6. The performance metrics in FS application, i.e., without the medium material, are also calculated, serving as the baseline for further comparison.

For the close contact scenario ($D = 0$), the loading of dielectric material shifts the resonant frequency of the array antenna to a lower frequency. The bigger the thickness, the larger the resonant frequency shifts. Hence, the degradation in radiation patterns can be observed in Fig. 2 clearly.

For most material loading scenarios, when the thickness of the material is approaching or equal to odd times of $0.25 \lambda_g$, i.e., $T = 0.25$ and $0.75 \lambda_g$ in this study,

there are obvious shifts in the resonant frequencies, degradations in the realized gain and distortions in the radiation patterns compared with those of FS scenarios.

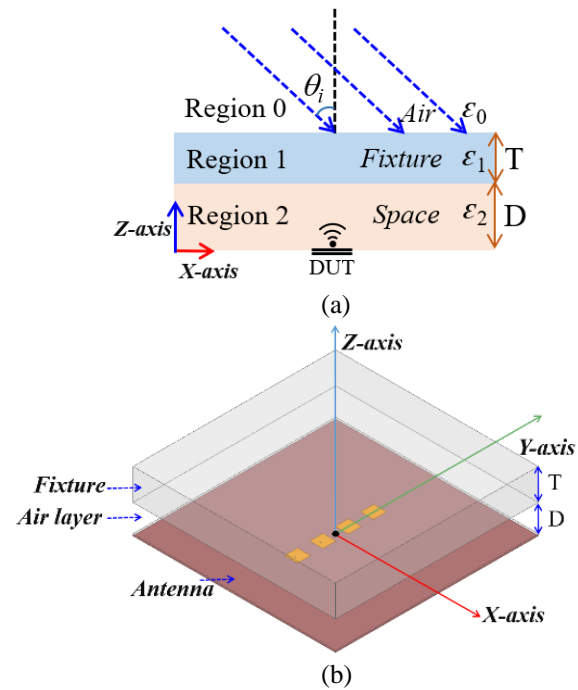
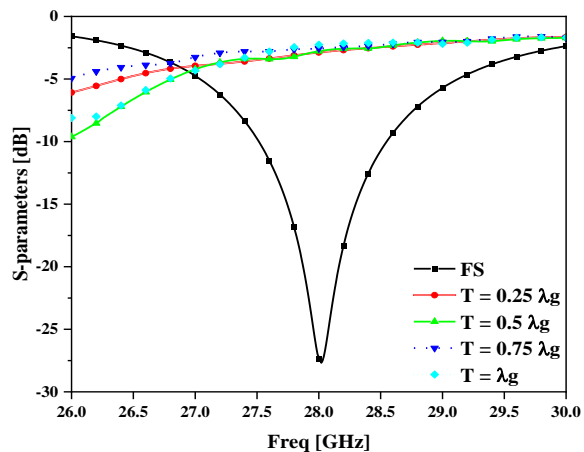


Fig. 1. (a) Schematic diagram of the fixture and DUT, and (b) tiled view of the antenna array and the fixture.

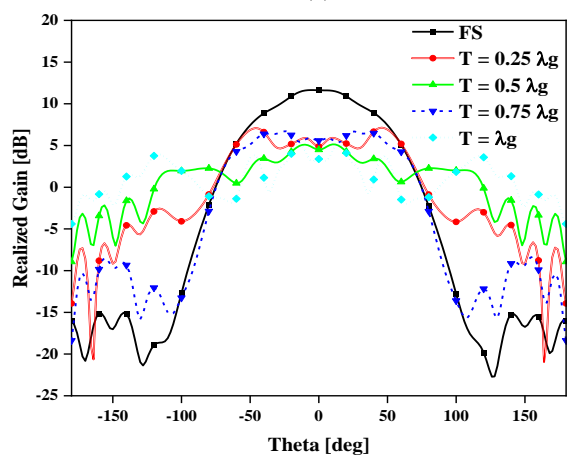
The material thickness around integer times of $0.5 \lambda_g$, i.e., $T = 0.5$ and $1 \lambda_g$ in this study, can result in resonant frequency and realized gain performance very close to those of FS scenarios.

There is also a very interesting phenomenon for the case of spacing between the array antenna and dielectric material approaching integer times of $0.5 \lambda_0$, i.e., $D = 0.5$ and $1 \lambda_0$, and the thickness of the material is approaching or equal to odd times of $0.25 \lambda_g$, i.e., $T = 0.25$ and $0.75 \lambda_g$ in this study, the focusing effect of noticeable higher realized gains and narrower main beams than those of FS case can be observed clearly. This can be explained that most rays emanating from the DUT going to free space will bend on the interface of different media and superpose in certain directions by proper arrangement of the layer parameters according to Snell's law.

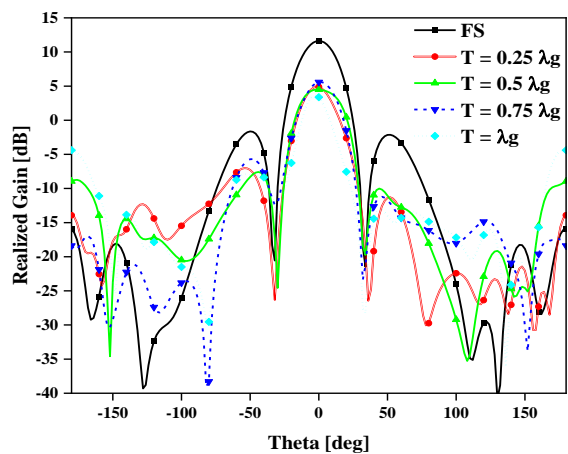
The above findings can be extended that not only in the broadside direction, but in any direction satisfying the corresponding combination conditions, changes in radiation performance can be observed. The specific reasons for the above conclusions refer to the next section.



(a)

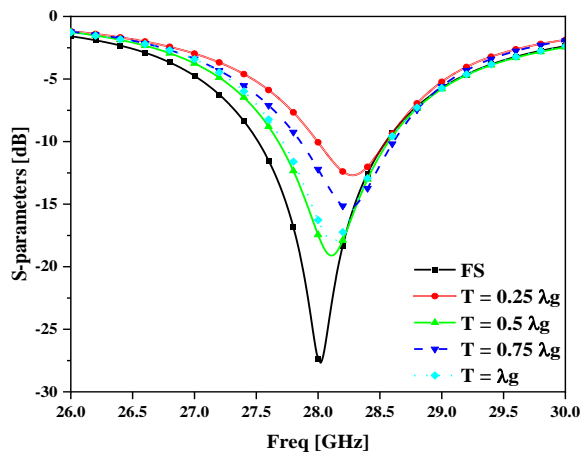


(b)

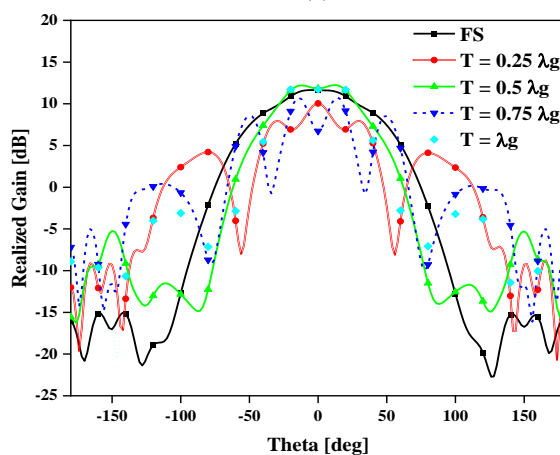


(c)

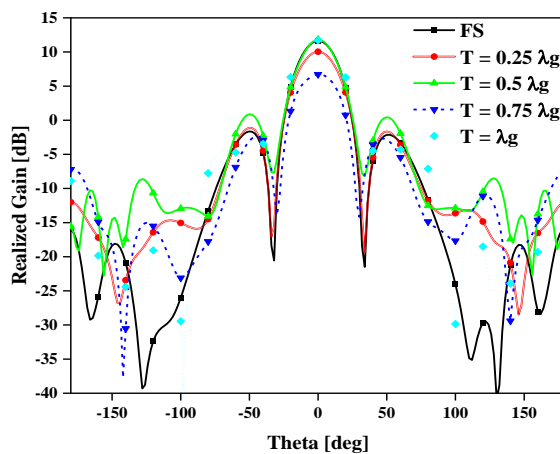
Fig. 2. Scattering parameters and radiation patterns for close contact ($D = 0$), (a) $|S_{11}|$, (b) pattern @ $\phi=0$, and (c) pattern @ $\phi=90$.



(a)



(b)



(c)

Fig. 3. Scattering parameters and radiation patterns for $D = 0.25 \lambda_0$, (a) $|S_{11}|$, (b) pattern @ $\phi=0$, and (c) pattern @ $\phi=90$.

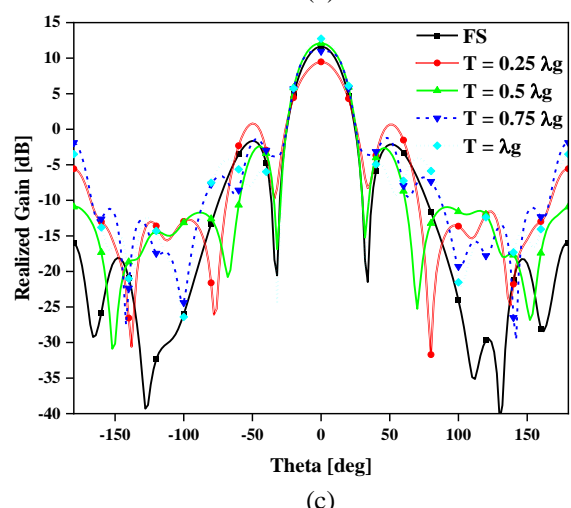
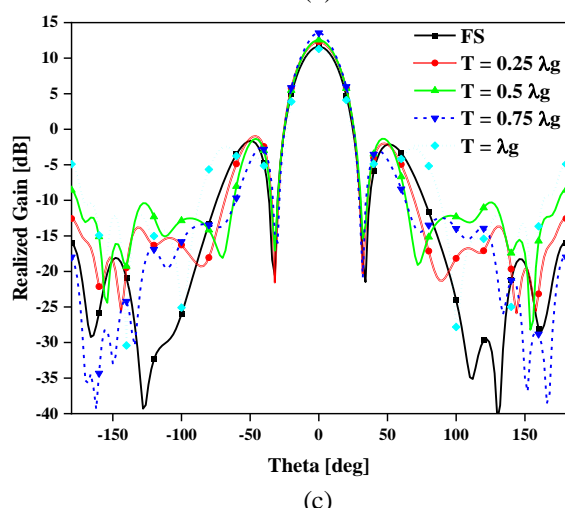
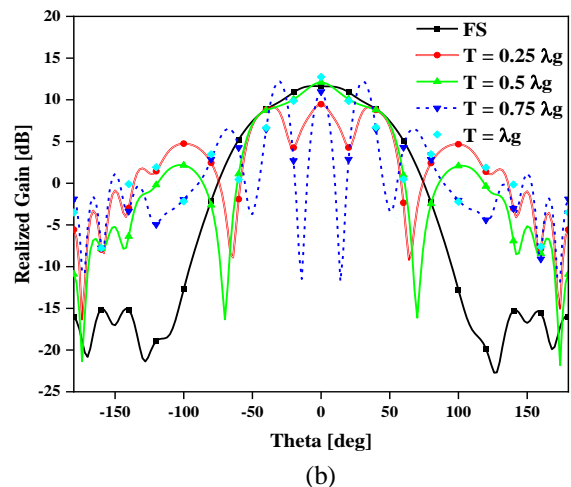
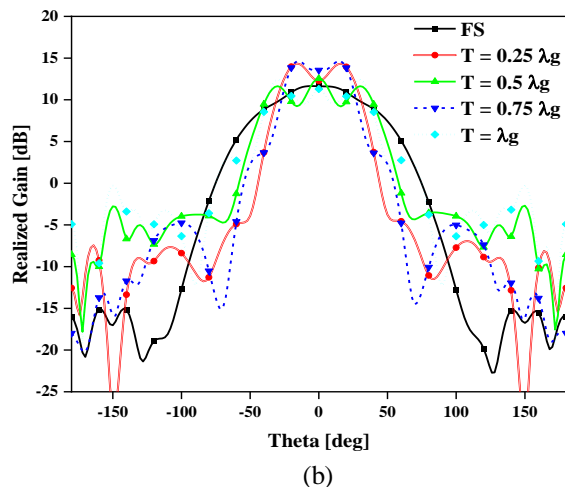
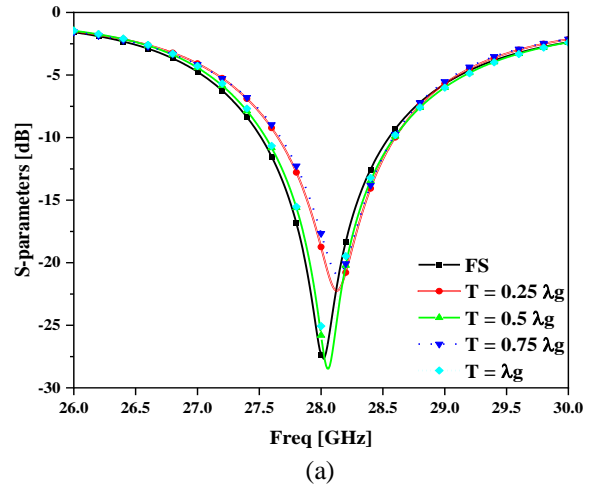
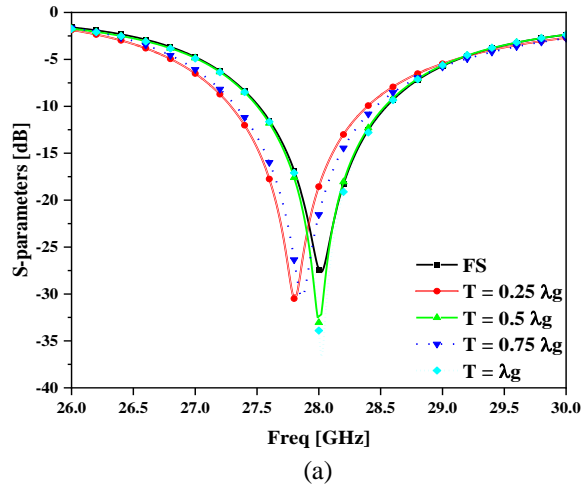
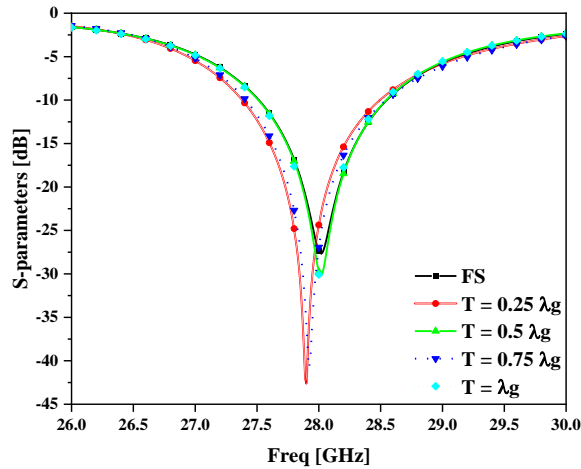
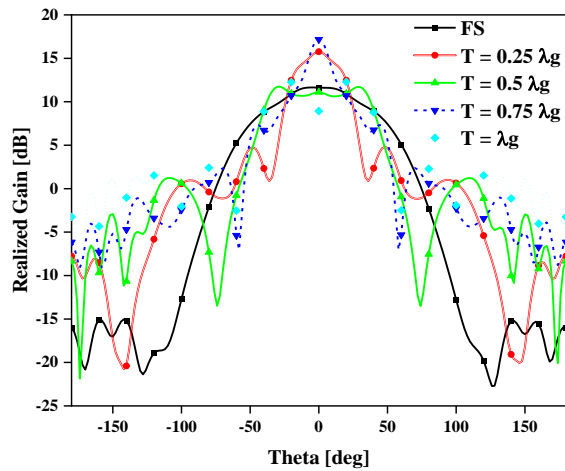


Fig. 4. Scattering parameters and radiation patterns for $D = 0.5 \lambda_0$, (a) $|S_{11}|$, (b) pattern @ $\phi=0$, and (c) pattern @ $\phi=90$.

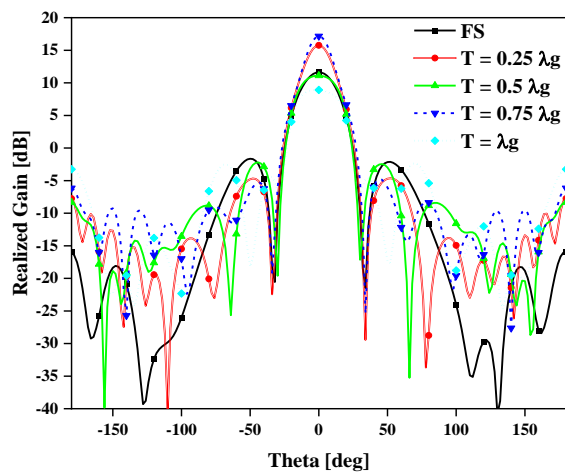
Fig. 5. Scattering parameters and radiation patterns for $D = 0.75 \lambda_0$, (a) $|S_{11}|$, (b) pattern @ $\phi=0$, and (c) pattern @ $\phi=90$.



(a)



(b)



(c)

Fig. 6. Scattering parameters and radiation patterns for $D = \lambda_0$, (a) $|S_{11}|$, (b) pattern @ $\phi=0$, and (c) pattern @ $\phi=90$.

III. PRINCIPLE OF FIXTURE AFFECTING MILLIMETER-WAVE DUT BASED ON TRANSMISSION LINE THEORY

To further understand the impact of the fixture on mm-Wave DUT radiation performance, this section analyzes its principle based on transmission line theory.

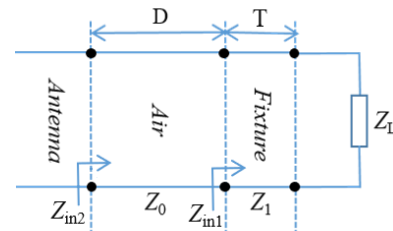


Fig. 7. Schematic diagram of the equivalent cascade transmission line.

Electromagnetic waves could propagate in the medium with a certain wave impedance which depends on the characteristic parameters of the medium (dielectric constant and permeability). The wave impedance of air is 377Ω . The whole propagation process can be equivalent to the cascade of several transmission lines with different characteristic wave impedances as can be seen from Fig. 7. The load impedance Z_L is equal to the wave impedance Z_0 in FS.

Cascade transmission lines can be regarded as a multistage impedance converter. According to the theory of transmission line, when the length of a transmission line is T and the characteristic impedance is Z_1 , the input impedance Z_{in1} of the transmission line terminated with load $Z_L = Z_0$ could be calculated by:

$$Z_{in1} = Z_1 \frac{Z_0 \cos(\beta T) + jZ_1 \sin(\beta T)}{Z_1 \cos(\beta T) + jZ_0 \sin(\beta T)}. \quad (1)$$

It can be derived:

$$T = 2k \cdot \lambda / 4, \quad Z_{in} = Z_0, \quad (2)$$

$$T = (2k-1) \cdot \lambda / 4, \quad Z_{in} = Z_1^2 / Z_0, \quad (3)$$

where β is a propagation constant, k is a nonzero integer. If the electromagnetic wave could propagate forward completely through the mounting structure and produce zero reflection, it is necessary to ensure impedance conjugate matching, that is, to meet the condition of Equation (2). At this time, the influence of the fixture on the electromagnetic wave is reduced to the minimum. Therefore, it is necessary to ensure that the electrical length of the transmission line is an integral multiple of π , that is to say, the thickness of the fixture (T) should be an integral multiple of the half dielectric wavelength, and the minimum thickness should be the half dielectric wavelength. This is consistent with the above simulated

results in Section II. Based on this, we recommend that for practical mounting fixture design, the thickness of the fixture should be integer times of $0.5 \lambda_g$.

When the length of T satisfies Equation (3), namely, T is odd times of $0.25 \lambda_g$, the fixture could transform 377Ω to Z_{12}/Z_0 . At this time, the condition of impedance matching is no longer satisfied, that is to say, the fixture has a reflection effect on the electromagnetic wave greatly. The electromagnetic wave reflected by the antenna surface experiences a 180° phase shift due to the fixture, which greatly affects the working frequency and radiation pattern of the mm-Wave antenna. Therefore, when the thickness of the material is approaching or equal to odd times of $0.25 \lambda_g$, the working frequency deviated seriously and the radiation pattern deteriorated clearly:

$$Z_{in2} = Z_0 \frac{Z_{in1} \cos(\beta D) + jZ_0 \sin(\beta D)}{Z_0 \cos(\beta D) + jZ_{in1} \sin(\beta D)}. \quad (4)$$

It can be calculated:

$$D = 2k \cdot \lambda / 4, \quad Z_{in2} = Z_{in1}, \quad (5)$$

$$D = (2k-1) \cdot \lambda / 4, \quad Z_{in2} = Z_0^2 / Z_{in1}. \quad (6)$$

If the spacing between the array antenna and fixture (D) as well as the thickness of the fixture (T) are set to integer times of $0.5 \lambda_0$ (meet Equations (2) and (5) in this case), under the condition of antenna resonance, each transmission component of the electromagnetic wave has the same phase value after passing through the fixture, which realizes in-phase superposition and continuous enhancement. At the same time, the reflection component decreases with the increase of reflection times due to the inverse effect [7-8].

We also analyze the phenomenon of antenna gain improvement (focusing) when the spacing between the array antenna and fixture (D) is integer times of $0.5 \lambda_0$ and the thickness of fixture (T) is odd times of $0.25 \lambda_g$ (meet Equations (3) and (5) in this case), which is obtained in Section II. Since the air layer between the antenna and the fixture is an integral multiple of the half wavelength, this is equivalent to the case where there is no air layer between the antenna and the fixture and is close to each other. Importantly, it should be mentioned that there is no gain improvement in FS when D equals zero. Only when D is integer times of $0.5 \lambda_0$ and T odd times of $0.25 \lambda_g$, can the gain improvement be achieved. However, it should be noted that this is a test error and does not represent the true gain of the antenna. This configuration should be avoided. The reason is like Fabry-Perot cavity antenna theory which is explained as follows:

Assuming that the reflection coefficient of the fixture is $\rho e^{j\phi}$, the radiation pattern of the DUT is $f(\alpha)$, n is the number of reflections, θ_n is the total phase difference between the beam reflected n times and the initial beam. If there is no loss in the transmission between the fixture and the DUT, the amplitude of the

electric field at the far field should be the vector superposition of multiple transmitted waves:

$$E = \sum_{n=0}^{\infty} f(\alpha) E_0 \rho^n \sqrt{1-\rho^2} e^{j\theta_n}. \quad (7)$$

Therefore, for the electromagnetic wave of antenna resonance frequency, the reflection is very small and the energy is almost transmitted. This phenomenon could improve the antenna gain, which could be applied to the design of high-gain antennas [9-12].

IV. CONCLUSION

To sum up, a truly FS configuration does not exist for 5G mm-Wave device OTA testing because they can't be floated in the air. It can be found that not only the property of the dielectric material imitating mounted fixtures, but also the spacing between DUT and fixtures, or the combination of them, will affect the measurements. We suggest that maybe white-box measurements are needed for mm-Wave DUTs in which the locations of mm-Wave modules are declared by manufacturers and the scanning ranges of which should not be covered or blocked by mounting fixtures. In addition, based on the findings in this study, for practical mounting fixture design, the thickness of the mounting structure should be close to integer times of $0.5 \lambda_g$ to minimize the impact of the fixture on DUTs. These proposals are for the original entrusted manufacturers (OEMs) and DUT mounting fixture vendors.

ACKNOWLEDGMENT

This research was funded in part by the Major State Basic Research Development Program (2019YFF0216600), and in part by the Fundamental Research Funds for the Central Universities (CUC210B012).

REFERENCES

- [1] Y. Niu, Y. Li, D. Jin, L. Su, and A. V. Vasilakos, "A survey of millimeter wave communications (mmWave) for 5G: opportunities and challenges," *Wireless Networks*, vol. 21, pp. 2657-2676, 2015.
- [2] H. Gamage, N. Rajatheva, and M. Latvaaho, "Channel coding for enhanced mobile broadband communication in 5G systems," *European Conference on Networks and Communications*, pp. 1-6, 2017.
- [3] S. G. Pannala, "Feasibility and challenges of over-the-air testing for 5G millimeter wave devices," in *2018 IEEE 5G World Forum (5GWF)*, pp. 304-310, 2018.
- [4] B. Derat, C. Rowell, and A. Tankielun, "Promises of near-field software and hardware transformations for 5G OTA," *IEEE Conference on Antenna Measurements Applications*, 2018.
- [5] H. Huang, "Overview of 5G mm-wave antenna design solutions in cellular phones: AiP, AiA, and

- AiAiP,” *International Symposium on Antennas and Propagation*, 2019.
- [6] CTIA, “Test Plan for Wireless Device Over-the-Air Performance,” 2019.
- [7] A. K. Gautam and M. Singh, “Design of gain enhanced stacked rectangular dielectric resonator antenna for C-band applications,” in *International Conference on Computing for Sustainable Global Development*, pp. 119-123, 2016.
- [8] Y. Pan and S. Y. Zheng, “A low-profile stacked dielectric resonator antenna with high-gain and wide bandwidth,” *IEEE Antennas and Wireless Propagation Letters*, vol. 15, pp. 68-71, 2016.
- [9] S. A. Muhammad, R. Sauleau, and H. Legay, “Purely metallic waveguide-fed Fabry–Perot cavity antenna with a polarizing frequency selective surface for compact solutions in circular polarization,” *IEEE Antennas and Wireless Propagation Letters*, vol. 11, pp. 881-884, 2012.
- [10] J. Ren, W. Jiang, K. Zhang, and S. Gong, “A high-gain circularly polarized Fabry–Perot antenna with wideband low-RCS property,” *IEEE Antennas and Wireless Propagation Letters*, vol. 17, pp. 853-856, 2018.
- [11] F. Deng and J. Qi, “Shrinking profile of Fabry–Perot cavity antennas with stratified metasurfaces: Accurate equivalent circuit design and broadband high-gain performance,” *IEEE Antennas and Wireless Propagation Letters*, vol. 19, pp. 208-212, 2020.
- [12] Y. Lv, X. Ding, and B. Wang, “Dual-wideband high-gain Fabry–Perot cavity antenna,” *IEEE Access*, vol. 8, pp. 4754-4760, 2020.



Xudong An Senior Engineer, Director of Antenna and Positioning Department, China Academy of Information and Communications Technology. He has long been engaged in the research and standardization of cellular mobile communication (3G, 4G, 5G, etc.), 5G terminal test technology, large-scale array antenna system, position-based technology, gesture recognition and test system development. He has published more than ten papers and articles in journals and conferences at home and abroad, and applied for 6 patents related to mobile communication equipment testing.



Meijun Qu received the Ph.D. degree from the School of Information and Communication Engineering, Beijing University of Posts and Telecommunications (BUPT), Beijing, China, in 2020. She is currently a Lecturer at Communication University of China, China. Her research interests include microwave passive component, antenna, meta-material, and electromagnetic compatibility.



Siting Zhu R & D Engineer, Antenna and Positioning Department, China Academy of Information and Communications Technology, is engaged in the research of MIMO OTA and 5G terminal test, standard setting and related technologies, participated in the National Science and Technology Major Special "R15-oriented 5G terminal test system and platform research and development," and other projects.



Xiaochen Chen Senior Engineer, Chinese Leaders of EU FP6 GO4IT, FP7 WALTER, is responsible for several national development and reform commission projects and major special sub-project research of the Ministry of Industry and Information Technology. He is responsible for formulating more than 20 domestic and foreign communication standards, applying for / owning 6 patents, and publishing more than 20 academic papers. Now, he works at China Telecommunication Technology Labs, China Academy of Information and Communication Technology, Beijing 100876 China.